

Original Article

Quantitative comparison between single-photon emission computed tomography and positron emission tomography imaging of lung ventilation with ^{99m}Tc-technegas and ⁶⁸Ga-gallgas in patients with chronic obstructive pulmonary disease: A pilot study

ABSTRACT

The aim of this study was quantitative comparison between ⁶⁸Ga-Gallgas positron emission tomography (PET) and ^{99m}Tc-Technegas single photon emission computed tomography (SPECT) for lung ventilation function assessment in patients with moderate-to-severe obstructive pulmonary disease and to identify image-derived texture features correlating to the physiologic parameters. Five patients with moderate-to-severe chronic obstructive pulmonary disease with PET and SPECT lung ventilation scans were selected for this study. Threshold-based segmentations were used to compare ventilated regions between both imaging techniques. Histograms of both scans were compared to reveal main differences in distributions of radiotracers. Volumes of segmentation as well as 50 textural features measured in the pulmonary region were correlated to the forced expiratory volume in 1 s (FEV1) as the relevant physiological variable. A better peripheral distribution of the radiotracer was observed in PET scans for three out of five patients. A segmentation threshold of 27% and 31% for normalized scans, for PET and SPECT respectively, was found optimal for volume correlation with FEV1. A high correlation (Pearson correlation coefficient >0.9) was found between 16 texture features measured from SPECT and 7 features measured from PET and FEV1. Quantitative measurements revealed different tracer distribution in both techniques. These results suggest that tracer distribution patterns may depend on the cause of the pulmonary obstruction. We found several texture features measured from SPECT to correlate to FEV1.

Keywords: Gallgas, quantification, technegas, texture features

INTRODUCTION

The severity of chronic obstructive pulmonary disease (COPD) is clinically diagnosed with spirometry by measuring forced expiratory volume in 1 s (FEV1). However, this measurement does not give any information about the obstructed regions in the lung. A better assessment of small airway diseases can be obtained with lung scintigraphy.^[1] Ventilation/perfusion (V/Q) single-photon emission computed tomography (SPECT) has also been incorporated for airway function diagnosis.^[2]

For regional lung obstruction imaging, tomographic three-dimensional (3D) images obtained in SPECT have a clear advantage over 2D projection images obtained in

**ENRIQUE GUSTAVO CUÑA, JUAN PABLO GAMBINI¹,
LILIANA SERVENTE², EDUARDO SAVIO²,
HENRY WILLIAM ENGLER²,
GABRIEL ADRIÁN GONZÁLEZ, OMAR ALONSO^{1,2}**

Physics Institute, Sciences Faculty, UDELAR, ¹Center for Nuclear Medicine, Clinics Hospital, Medicine Faculty, UDELAR, ²Uruguayan Center for Molecular Imaging, CUDIM, Montevideo, Uruguay


Address for correspondence: Mr. Enrique Gustavo Cuña, Dr. Américo Ricaldoni 2010, Montevideo, Uruguay.
E-mail: enriquecuna@gmail.com

This is an open access journal, and articles are distributed under the terms of the Creative Commons Attribution-NonCommercial-ShareAlike 4.0 License, which allows others to remix, tweak, and build upon the work non-commercially, as long as appropriate credit is given and the new creations are licensed under the identical terms.

For reprints contact: reprints@medknow.com

How to cite this article: Cuña EG, Gambini JP, Servente L, Savio E, Engler HW, González GA, *et al.* Quantitative comparison between single-photon emission computed tomography and positron emission tomography imaging of lung ventilation with ^{99m}Tc-technegas and ⁶⁸Ga-gallgas in patients with chronic obstructive pulmonary disease: A pilot study. *World J Nucl Med* 2019;18:251-7.

Submission: 02-May-18, **Accepted:** 13-Jul-18

Access this article online	
Website: www.wjnm.org	Quick Response Code 
DOI: 10.4103/wjnm.WJNM_45_18	

scintigraphy. Technegas (Cyclomedica Ltd.) is used to assess lung ventilation function.^[3] Technegas is a pseudo-gas, consisting of carbon nanoparticles suspended in argon and labeled with ^{99m}Tc. The size of carbon nanoparticles is about 100–300 nm. This allows for pulmonary ventilation imaging in nearly physiological conditions, since nanoparticles can reach the alveolar space.^[2]

As an alternative to SPECT, studies have reported the feasibility and implementation of Gallgas-positron emission tomography (PET) scans for lung ventilation.^[4-7] Gallgas is a radiotracer made with the same carbon nanoparticles as Technegas but labeled with ⁶⁸Ga. Gallium-68 is an attractive PET radionuclide due to its short half-life (~68 min), ease of production, availability, and compatibility with medical applications.^[8,9] Qualitative comparison studies between Technegas-SPECT and Gallgas-PET have been reported,^[10] where Gallgas PET shows a better distribution inside the lungs providing a better visualization of ventilation heterogeneities. Other comparative studies have shown that diagnoses with Technegas-SPECT and Gallgas-PET are compatible most of the time; however, PET offers more confidence diagnosis in some cases.^[6]

It is well known that PET has better spatial resolution than SPECT.^[11] However, SPECT has the potential to become a more sophisticated technology through image analysis techniques.^[2] On the other hand, PET is gaining relevance in diagnose of pulmonary imaging^[12] and will most likely continue to be used for this purpose in the future. For these reasons, we considered a quantitative comparison between Gallgas-PET and Technegas-SPECT to be of interest.

Previous authors have investigated the feasibility of selecting obstructed lung regions in the lungs using textural features calculated from computed tomography (CT) images.^[13] They found that a very good agreement with the segmentation obtained through texture features' quantification and visual assessment done by experienced physicians.

We hypothesize that quantification in both techniques is relevant for diagnostic/prognostic purposes. Moreover, advanced quantitative parameters such as texture features, measured from ventilation PET and SPECT scans, are likely to show correlations to FEV1 as the physiologic variable used to assess COPD severity.

SUBJECTS AND METHODS

Patients

This study was approved by the Institutional Review Board and all participants signed an informed consent form. For

this retrospective study, five patients with appropriate nonattenuation-corrected Gallgas-PET scans and available Technegas nonattenuation-corrected SPECT scans were selected. Nonattenuation correction scans were used to compare PET to SPECT acquisition mode. All these patients had moderate-to-severe COPD and underwent Gallgas-PET scans at our center between September 2011 and July 2012. PET and SPECT scans were performed within 4 days of each other. Table 1 shows the details for the patients.

Radiopharmaceutical production

Technetium ^{99m} was obtained from a ⁹⁹Mo/^{99m}Tc generator. For gallium-68, an eluate from a ⁶⁸Ge/⁶⁸Ga generator was purified and concentrated by a QMA cartridge before production of Gallgas nanoparticles. In both cases, carbon nanoparticles were produced with a commercial device from Cyclomedica Ltd. Both radioisotopes were bound to carbon particles in a pure argon atmosphere and a temperature of 2500°C. For Gallgas, carbon nanoparticles were labeled with ⁶⁸Ga as GaCl₃. For Technegas, nanoparticles were labeled with ^{99m}Tc as ^{99m}TcO₄⁻.

Imaging

An estimated mean inhaled activity of 70 MBq for Technegas and 27 MBq for Gallgas was administered to the patients, instants before scanning. Ventilation SPECT was performed acquiring 120 images around a 360° angle, with 15 s per step. Gallgas PET/CT was performed using 2 or 3 bed positions, 3 min each, with a 64-slice multidetector CT component. Each bed position comprises 46 slices. A bed overlap of 11 slices was used (approximately 24%). Both images were reconstructed using an iterative OSEM algorithm. PET images were corrected using time of flight.

Region of interest definition

The analyzed voxels from PET and SPECT scans were limited to the pulmonary region. This region-of-interest (ROI) was segmented using the inspiration CT images and extrapolated to PET and SPECT scans. All ROIs underwent visual inspection for further verification. Trachea and main bronchus regions were removed manually from the ROI.

Image analysis

SPECT data were not corrected for attenuation, since it was acquired using a dedicated SPECT camera. To compare both

Table 1: Details of patient cohort

Patients	Diagnose	Age	Sex
1	Bullous emphysema	48	Female
2	Panlobular emphysema	55	Male
3	Chronic bronchitis	74	Male
4	Emphysema	61	Male
5	Diffuse panlobular emphysema	37	Male

imaging techniques, we used the nonattenuation-corrected PET data. SPECT scans were rigidly registered to PET using normalized mutual information maximization criteria. After rigid registration, SPECT scans data grid sizes were resampled to PET scans' data grids using nearest-neighbor interpolation method.

Volume segmentation

Threshold-based segmentation was performed by taking into account voxels with values within a fixed range from SPECT and PET scan data. Pearson's correlation coefficients between segmented volumes and FEV1 were calculated to find optimal segmentation thresholds. Voxel histograms were calculated considering voxels inside the segmented pulmonary region. For these voxels, an estimated value for background activity was calculated using the mean value of voxels from the surrounding area outside the lungs. Voxels with values lower than background were not considered for the histograms.

Texture features

Texture features were measured from PET and SPECT scans. To quantify these values, we calculated parametric maps from scans using patches. A patch is defined as a cube with $N \times N \times N$ voxels (N-patch) centered in a single voxel. To obtain a parametric map, each voxel is replaced by the value of a single feature calculated inside the N-patch centered in that voxel. The final result is a 3D volume with the same size as the scan data, each parametric map corresponds to a single texture feature. In this case, we used a 5-patch size for calculations.

To assign a feature a value from a given ROI, the mean value of the corresponding parametric map voxels inside this ROI is calculated. Voxels with neighboring patches that fell outside the pulmonary region were not taken into account.

Fifty different first, second, and higher order texture features were calculated from tomographic PET and SPECT scans.

First-order features: mean (1), median (2), variance (3), coefficient of variation (4), skewness (5), kurtosis (6), energy (7), and entropy (8).^[14]

Second-order features from gray level co-occurrence matrix: angular moment (9), contrast (10), correlation (11), sum of square variance (12), inverse difference moment (13), sum average (14), sum variance (15), sum entropy (16), entropy (17), difference variance (18), difference entropy (19), information measure of correlation (20 and 21), maximum correlation coefficient (22), maximal probability (23), diagonal moment (24), dissimilarity (25), difference energy (26),

inertia (27), inverse difference moment (28), sum energy (29), cluster shade (30), and cluster prominence (31).^[15]

High-order features using gray level run length matrix: short run emphasis (32), long run emphasis (33), gray-level nonuniformity (34), run length nonuniformity (35), run percentage (36), low gray-level run emphasis (37), high gray-level run emphasis (38), short-run low gray-level emphasis (39), short-run high gray-level emphasis (40), long run low gray-level emphasis (41), and long run high gray-level emphasis (42).^[16]

High-order features using neighboring gray level dependence matrix: small number emphasis (43), large number emphasis (44), number nonuniformity (45), second moment (46), and entropy (47).^[17]

High-order features using neighboring gray-tone difference matrix: coarseness (48), contrast (49), and busyness (50).^[18]

Correlations between texture feature segmentation and forced expiratory volume in 1 s

Using the previously described parametric maps, we used threshold-based segmentation to divide voxels inside the lung region. We measured Pearson's correlation coefficients between the total volume of the segmented regions and FEV1 volumes, for all 50 texture features, after proper standardization of features' quantitative values. The highest Pearson's correlation coefficient was used as criteria to find optimal segmentation threshold using texture features.

Statistical comparison between texture features

Using the optimal segmentation thresholds measured from PET and SPECT, we selected the voxels inside the obstruction regions common to both techniques. Thus, we took into consideration voxels corresponding to obstructed regions for both PET and SPECT scans. We compared the mean and variance values for each texture feature from all these voxels taken from all five patients to compare SPECT and PET features.

All image analysis, quantification, and statistic tests were done using the software MATLAB release 2017a (The MathWorks, Inc., Natick, Massachusetts, United States).

RESULTS

Correlation coefficients between FEV1 and segmented volumes for several thresholds are shown in Figure 1. Maximum correlation coefficient values are obtained for a threshold of 27% of maximum uptake for PET and 31% of maximum uptake for SPECT scans, with Pearson's correlation coefficients of 0.90 ($P = 0.039$) and 0.98 ($P = 0.002$), respectively.

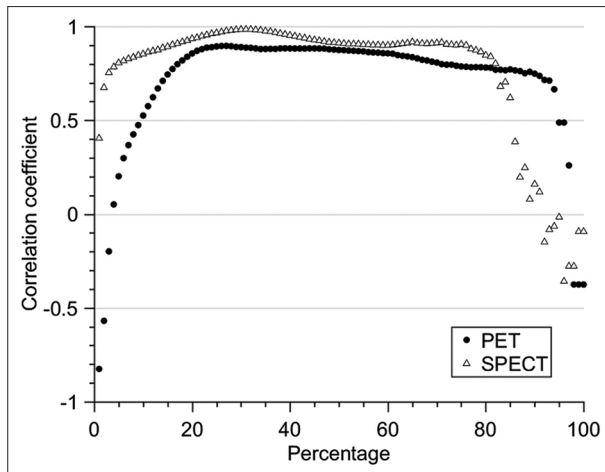


Figure 1: Correlation coefficients between threshold-segmented volumes and forced expiratory volume in 1 s

The histograms measured for each patient, from PET and SPECT scans, and the intensity volume histograms (IVHs) are shown in Figure 2. IVH shows the volume in liters taking into account all the voxels with values above a given threshold as a percentage of maximum uptake. Figure 3 shows maximum intensity projections of PET and SPECT scans limited to the lung regions for all five patients in the study.

Segmentation volumes using some of the 50 different texture features were found to show high Pearson's correlation coefficients (>0.9) when compared to FEV1 as the physiologic variable. These features, their corresponding threshold values for segmentation, together with correlation coefficients and their *P* values are shown in Tables 2 and 3 for Gallgas-PET and Technegas-SPECT, respectively.

Mean and standard deviation values of voxels inside obstructed lung regions were calculated from parametric maps corresponding to these features, for both Technegas-SPECT and Gallgas-PET scans. Comparison bar graphs for mean and standard deviation can be seen in Figures 4 and 5, respectively.

DISCUSSION

FEV1 is the clinical quantitative variable generally used to assess COPD severity, this is why we used these values to find a correlation with lung ventilation volumes and thus obtain a significant threshold for segmentation in PET and SPECT scans. Optimal thresholds (as percentages of maximum voxel value) used to segment ventilation volumes were similar for PET and SPECT scans (27% and 31%, respectively). Previous studies analyzed the relationship between V/Q ratio and FEV1.^[19,20] In this case, we analyzed correlations between ventilation scans and FEV1. A correlation with a larger

Table 2: Texture features used for segmentation in positron emission tomography scans for which resulting volumes show high correlation with forced expiratory volume in 1 s

Feature (n)	Threshold	Pearson coefficient	<i>P</i>
3	32	0.96	0.011
5	52	0.91	0.031
10	86	0.94	0.018
23	76	0.93	0.02
27	86	0.94	0.012
31	91	0.97	0.005
35	81	0.98	0.004

Table 3: Texture features used for segmentation in single-photon emission computed tomography scans for which resulting volumes show high correlation with forced expiratory volume in 1 s

Feature (n)	Threshold	Pearson coefficient	<i>P</i>
1	43	0.97	0.006
2	39	>0.99	0.0001
3	18	0.97	0.006
4	71	0.97	0.005
8	92	0.9	0.036
12	51	>0.99	0.0003
14	65	0.98	0.004
16	100	0.95	0.014
17	98	0.95	0.014
19	99	0.96	0.011
29	49	0.97	0.006
33	53	>0.99	0.0001
34	96	0.97	0.008
36	99	0.96	0.01
38	85	0.97	0.006
41	53	>0.99	0.0003
43	96	0.95	0.012
50	49	0.98	0.003

patient cohort between ventilation-segmented volumes and FEV1 could reveal a link between tracer distribution and this physiological uptake. Visual inspection shows that the uptake regions above this threshold correspond to what would be visually assigned to the ventilated regions of the lungs. Figure 6 shows the ventilated regions calculated using these thresholds in the same slice of the same patient using PET and SPECT (images have been fused with CT for clarity).

In an attempt to characterize tracer distribution, we plotted histograms and IVHs from PET and SPECT scans and compared them for each one of our five patients. Comparisons between histograms from PET and SPECT show similarities in some regions, but most of them show differences for a given range of voxel values. These histograms are complemented by the IVHs. Regions where histograms show more voxel counts in PET, together with the higher level of the IVH curves translate the fact that there is a better peripheral distribution of Gallgas

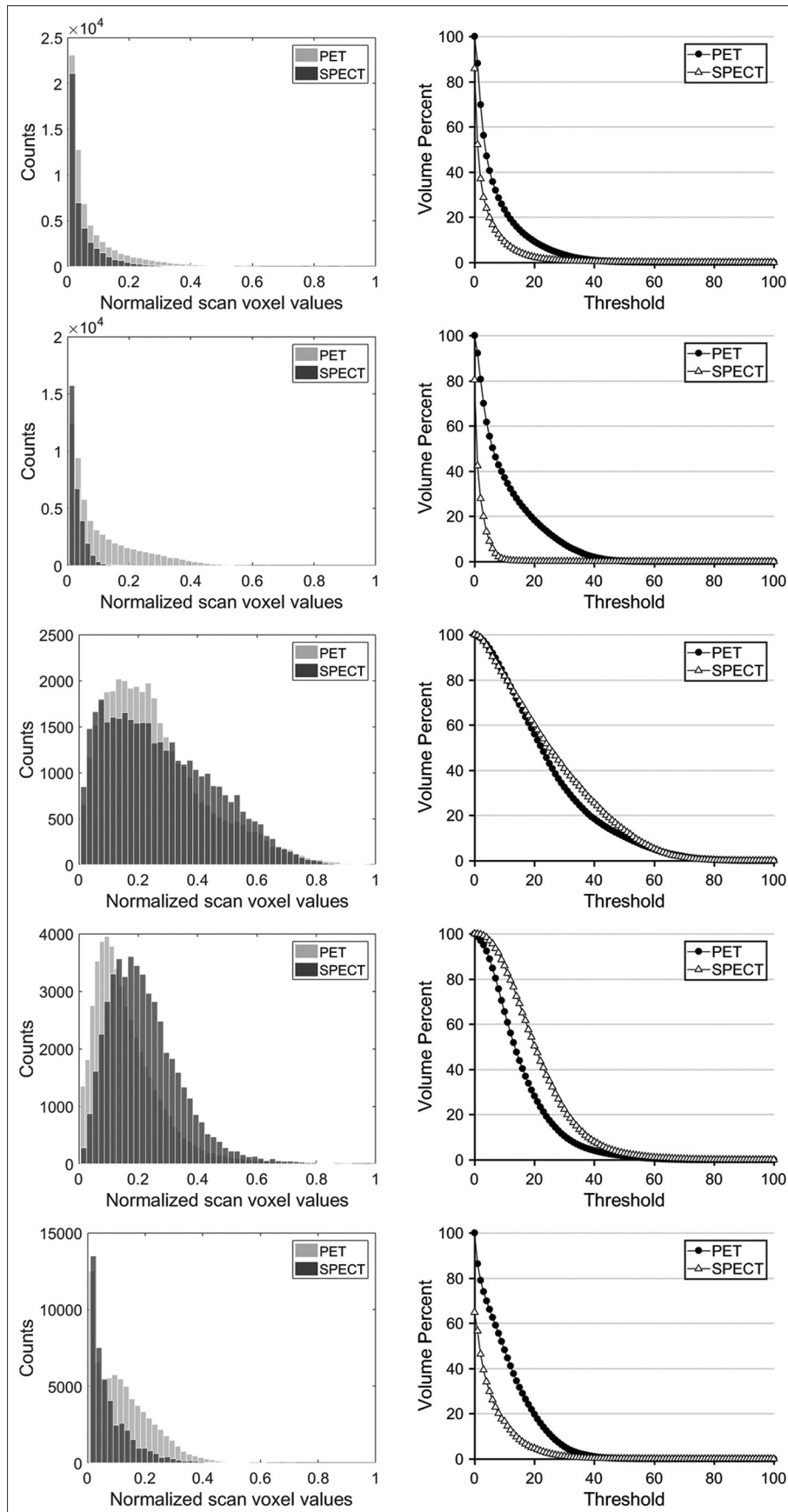


Figure 2: Comparison between histograms of positron emission tomography and single-photon emission computed tomography scans (first column) and intensity volume histograms (second column), for each patient

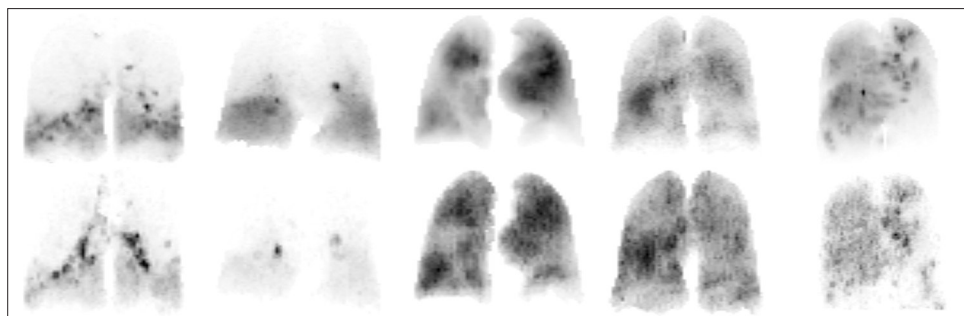


Figure 3: Normalized voxel values positron emission tomography (top row) and single-photon emission computed tomography (bottom row) maximum intensity projection scans. Each column corresponds to scans for the same patient

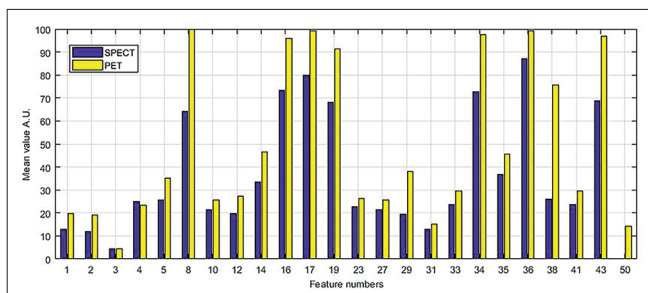


Figure 4: Mean values for the features with which segmentation volumes exhibit high correlation with forced expiratory volume in 1 s, inside obstructed lung regions

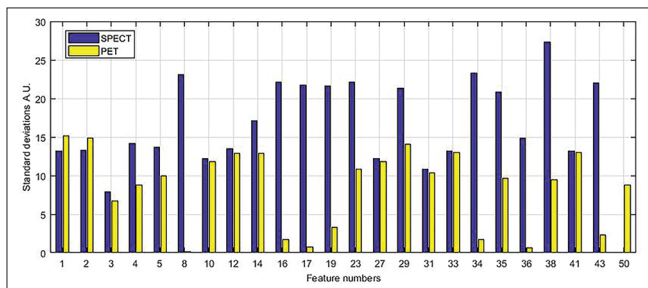


Figure 5: Standard deviations for the features with which segmentation volumes exhibit high correlation with forced expiratory volume in 1 s, inside obstructed lung regions

when compared to Technegas. This is the other reason why we used nonattenuation-corrected scans, to see more peripheral distribution of the tracer in the lungs. Interestingly, even if three of the cases in this study showed the same tendency, the other two showed an opposite, yet less marked, behavior. This suggests that the radiopharmaceutical distribution could strongly depend on the cause of pulmonary disease and the used radiotracer (in pseudogas form).

Texture features are useful when they can be related and used to assess certain aspects of patient clinical data. In this case, we used textural features for threshold-based segmentations using both SPECT and PET data in the lung tissues. Textural features in the lungs have been studied as measured from CT scans.^[13] To the best of our knowledge, there are no studies

where textural features have been quantified using SPECT or PET scans for lung ventilation. We chose a patch size of $5 \times 5 \times 5$ voxels, which by the voxel size accounts for 2.5 cm, as we considered this to be large enough for the features not to be greatly affected by respiratory motion. Nevertheless, it would be interesting to conduct sensitivity studies with a larger patient sample and perform gated acquisitions. The segmented volumes we obtained showed a good correlation to FEV1 volumes for 18 features in SPECT and 7 features in PET. This suggests that there are intrinsic differences between the features measured in the obstructed and ventilated uptake regions of the lungs, in both SPECT and PET, and that textural features could play an important role in lung parenchyma segmentation using these imaging modalities. Furthermore, as we can see in Figures 4 and 5, some features exhibit similar statistical distributions in SPECT and PET scans. We think that a standardized protocol could provide more robust texture feature quantification in both techniques, as they seem to be consistent between these two scanning modalities. Although these measurements should be taken with caution as we have only a few patients, these results are encouraging to continue with similar trials.

CONCLUSION

To the best of our knowledge, this is the first study analyzing the differences between PET and SPECT using quantitative metrics other than standardized uptake value and V/Q. Taking this small cohort of patients into consideration, results suggest that tracer distributions could strongly depend on the cause of the disease. Segmentation using some texture features quantified from SPECT and PET was found to have a better correlation to physiological variable FEV1, motivating to continue the research in this field. Studies including a larger cohort of patients are necessary to have statistically significant results.

Acknowledgement

Authors would like to thank the graduate academic commission (CAP) for supporting graduate level research.

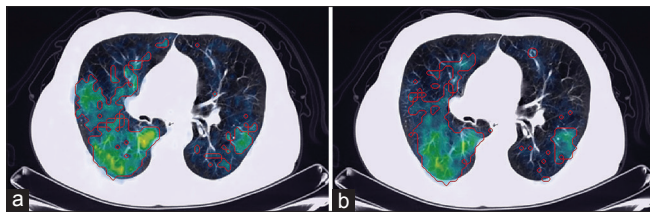


Figure 6: single-photon emission computed tomography segmentation of ventilated region with a threshold of 31% over the single positron emission computed tomography scan fused with the computed tomography (a). Positron emission tomography scan segmentation of ventilated region with a threshold of 27% over the positron emission tomography fused with the computed tomography (b)

Financial support and sponsorship

Funding from participating institutions.

Conflicts of interest

There are no conflicts of interest.

REFERENCES

1. Bajc M, Markstad H, Jarenbäck L, Tufvesson E, Bjermer L, Jögi J, *et al.* Grading obstructive lung disease using tomographic pulmonary scintigraphy in patients with chronic obstructive pulmonary disease (COPD) and long-term smokers. *Ann Nucl Med* 2015;29:91-9.
2. Schembri GP, Roach PJ, Bailey DL, Freeman L. Artifacts and anatomical variants affecting ventilation and perfusion lung imaging. *Semin Nucl Med* 2015;45:373-91.
3. Jögi J, Jonson B, Ekberg M, Bajc M. Ventilation-perfusion SPECT with ^{99m}Tc-DTPA versus technegas: A head-to-head study in obstructive and nonobstructive disease. *J Nucl Med* 2010;51:735-41.
4. Alonso O, Gambini JP, Balter H, Nuñez M, Savio E, Paolino A, *et al.* PET lung ventilation scanning with gallium-68 aerosol (Galligas) versus technegas SPECT in patients with obstructive lung disease: A feasibility study. *J Nucl Med* 2012;53:2502.
5. Kipritidis J, Siva S, Hofman MS, Callahan J, Hicks RJ, Keall PJ, *et al.* Validating and improving CT ventilation imaging by correlating with ventilation 4D-PET/CT using ⁶⁸Ga-labeled nanoparticles. *Med Phys* 2014;41:011910.
6. Hofman MS, Beauregard JM, Barber TW, Neels OC, Eu P, Hicks RJ, *et al.* ⁶⁸Ga PET/CT ventilation-perfusion imaging for pulmonary embolism: A pilot study with comparison to conventional scintigraphy. *J Nucl Med* 2011;52:1513-9.
7. Kotzerke J, Andreeff M, Wunderlich G, Wiggermann P, Zöphel K. Ventilation-perfusion-lungscintigraphy using PET and ⁶⁸Ga-labeled radiopharmaceuticals. *Nuklearmedizin* 2010;49:203-8.
8. Decristoforo C. Gallium-68 – A new opportunity for PET available from a long shelf-life generator – Automation and applications. *Curr Radiopharm* 2012;5:212-20.
9. Dolovich MB, Bailey DL. Positron emission tomography (PET) for assessing aerosol deposition of orally inhaled drug products. *J Aerosol Med Pulm Drug Deliv* 2012;25 Suppl 1:S52-71.
10. Borges JB, Velikyan I, Långström B, Sörensen J, Ulin J, Maripuu E, *et al.* Ventilation distribution studies comparing technegas and “Galligas” using ⁶⁸GaCl₃ as the label. *J Nucl Med* 2011;52:206-9.
11. Spanoudaki VC, Ziegler SI. *PET & SPECT Instrumentation*. München: Springer; 2008.
12. Oehme L, Zöphel K, Golgor E, Andreeff M, Wunderlich G, Brogsitter C, *et al.* Quantitative analysis of regional lung ventilation and perfusion PET with (⁶⁸Ga)-labelled tracers. *Nucl Med Commun* 2014;35:501-10.
13. Chabat F, Yang GZ, Hansell DM. Obstructive lung diseases: Texture classification for differentiation at CT. *Radiology* 2003;228:871-7.
14. Gonzalez RC, Woods RE. *Digital Image Processing*. 3rd ed. Upper Saddle River (NJ): Pearson Prentice Hall; 2008.
15. Haralick RM, Shanmugan K, Dinstein I. Textural features for image classification. *IEEE Trans Syst Man Cybern* 1973;3:610-21.
16. Tang X. Texture information in run-length matrices. *IEEE Trans Image Process* 1998;7:1602-9.
17. Sun C, Wee WG. Neighboring gray level dependance matrix for texture classification. *Comput Vis Graph Image Process* 1982;23:341-52.
18. Amadasun M, King R. Textural features corresponding to textural properties. *IEEE Trans Syst Man Cybern* 1989;19:1264-74.
19. Le Roux PY, Siva S, Steinfors DP, Callahan J, Eu P, Irving LB, *et al.* Correlation of ⁶⁸Ga ventilation-perfusion PET/CT with pulmonary function test indices for assessing lung function. *J Nucl Med* 2015;56:1718-23.
20. Le Roux PY, Siva S, Callahan J, Claudic Y, Bourhis D, Steinfors DP, *et al.* Automatic delineation of functional lung volumes with ⁶⁸Ga-ventilation/perfusion PET/CT. *EJNMMI Res* 2017;7:82.